Julia Körner*, Christopher F. Reiche, Bernd Büchner, and Thomas Mühl

Theory and application of a novel co-resonant cantilever sensor

Theorie und Anwendung eines neuartigen ko-resonanten Cantilever-Sensors

Abstract: Dynamic cantilever sensors have many applications, for example in material's research, biology, as gas and magnetic field sensors. The sensing principle is based on the effect that a force gradient or mass change applied to the cantilever alter its oscillatory state which can be related to the parameter of interest. In order to detect very small interactions, the cantilever needs to have a low stiffness which is commonly achieved by a reduction of the beam's dimensions, especially its thickness. However, this is limited by the commonly employed laser-based detection of the cantilever's oscillatory state.

In this paper, we describe a novel co-resonant cantilever sensor concept which is based on the coupling and eigenfrequency matching of a micro- and a nanocantilever. This approach allows to access a large fraction of the nanocantilever's high sensitivity while ensuring a reliable oscillation detection with standard laser-based methods at the microcantilever. Experiments in cantilever magnetometry and magnetic force microscopy demonstrate the immense potential of the sensor concept. Furthermore, applications are not limited to material's research, instead this concept creates a cantilever sensor platform with many potential applications, for example as gas, mass or pressure sensors.

Zusammenfassung: Dynamische Cantilever-Sensoren werden vielfältig eingesetzt, zum Beispiel in der Materialforschung, zur Untersuchung biologischer Proben, als Gas- und Magnetfeldsensoren. Das Sensorprinzip basiert darauf, dass der Schwingungszustand des Cantilevers durch äußere Einflüsse, d.h. Kraftgradienten oder Massen, verändert wird, und daraus kann auf die Messgröße geschlossen werden. Zur Messung sehr kleiner Interaktionen werden möglichst weiche Federbalken eingesetzt. Eine geringe Federkonstante des Cantilevers wird im Allgemeinen durch einen Verringerung seiner Abmessung, insbesondere der Dicke, erreicht. Diese Optimierung des Sensors für die Messung kleinster Kräfte, Kraftgradienten und Massen ist jedoch dadurch begrenzt, dass für eine zuverlässige Schwingungsdetektion Laser-basierte Methoden eingesetzt werden.

Im folgenden Artikel wird ein neuartiges ko-resonantes Konzept für Cantilever-Sensoren vorgestellt, welches auf der Kopplung und Eigenfrequenz-Anpassung eines Mikro- und eines Nanocantilevers basiert. Mit diesem Ansatz wird ein großer Teil der hohen Empfindlichkeit des Nanocantilevers zugänglich, während gleichzeitig eine zuverlässige Schwingungsdetektion mit den bekannten Laser-optischen Methoden gewährleistet ist. In Experimenten in Cantilever Magnetometrie und Magnetkraftmikroskopie wurde das große Potential dieses Konzeptes gezeigt. Anwendungen beschränken sich aber nicht auf die Materialforschung, sondern das Konzept ist dafür geeignet, eine Cantilever-Sensor-Plattform zu schaffen, die für verschiedenste Anwendungen eingesetzt werden kann, zum Beispiel in der Gassensorik, als Massen- oder Drucksensor.

*Corresponding author: Julia Körner, Leibniz Institute for Solid State and Materials Research IFW Dresden, Helmholtzstr. 20, 01069 Dresden, Germany; and Department of Electrical and Computer Engineering, University of Utah, 50 Central Campus Dr Suite 2110, Salt Lake City, UT-84112, USA, e-mail: julia.koerner2k@gmail.com
Christopher F. Reiche, Leibniz Institute for Solid State and Materials Research IFW Dresden, Helmholtzstr. 20, 01069 Dresden, Germany; and Department of Electrical and Computer Engineering, University of Utah, 50 Central Campus Dr Suite 2110, Salt Lake City, UT-84112, USA
Bernd Büchner, Leibniz Institute for Solid State and Materials Research IFW Dresden, Helmholtzstr. 20, 01069 Dresden, Germany; and Institut für Festkörperphysik, Technische Universität Dresden, 01062 Dresden, Germany; and Center for Transport and Devices of Emergent Materials, Technische Universität Dresden, 01062, Dresden, Germany
Thomas Mühl, Leibniz Institute for Solid State and Materials Research IFW Dresden, Helmholtzstr. 20, 01069 Dresden, Germany; and Center for Transport and Devices of Emergent Materials, Technische Universität Dresden, 01062, Dresden, Germany

1 Introduction

Dynamic cantilever sensors are widely used in the fields of material's research, biology or as gas sensors [1, 2, 3, 4, 5, 6, 7]. In many cases, a one-side clamped beam is employed which is driven to oscillate at or close to its resonance frequency. Any interaction on the cantilever, e. g. force gradient or mass change, alters the beam's oscillatory state which is usually detected by laser-based methods. This change of the oscillatory state is used to derive the properties of the sample under investigation. For each of its eigenfrequencies, the cantilever can be described by a harmonic oscillator model [8] which consists of an effective cantilever mass m_{eff}, a damping element d and a spring k. By assuming that an external force gradient applied to the cantilever is represented by an additional spring Δk and that the effective cantilever mass stays unchanged, the eigenfrequency f_0 of the first flexural cantilever mode is [9]:

$$f_0^{\Delta k} = \frac{1}{2\pi} \sqrt{\frac{k + \Delta k}{m_{eff}}}. \tag{1}$$

Consequently, the frequency shift Δf_0 induced by the interaction can be approximated by:

$$\Delta f_0 = f_0^{\Delta k} - f_0 \approx \frac{f_0}{2k} \Delta k. \tag{2}$$

As equation (2) indicates, the frequency shift for a certain external influence and, hence, the sensitivity is mainly determined by the cantilever's stiffness. Please note that similar considerations can be made in order to evaluate the frequency shift associated with a mass change.

In order to extend the application range for these sensors to very small interactions, it is therefore a main goal to increase the sensitivity by reduction of the beam's spring constant. This can be achieved by decreasing cantilever size, especially its thickness, as the following expression for the static spring constant k of a cantilever with constant cross section indicates:

$$k = \frac{3EI}{L^3}. \tag{3}$$

Here E denotes Young's modulus, I the second moment of area and L the cantilever length. Please note that equation (3) is also a very good approximation for the dynamic spring constant of the first flexural cantilever mode which will be considered in the following. Assuming a rectangular cross section (width w, thickness t) as an example, the second moment of area is $I = 1/12 \cdot wt^3$, hence the spring constant reads:

$$k = \frac{Ewt^3}{4L^3}. \tag{4}$$

These considerations lead to the design of cantilevers where at least two out of three dimensions (thickness and width) are nanosized.

While this measure increases the sensitivity, it, at the same time, creates the challenge of reliably detecting the nanocantilever's oscillatory state. The commonly used laser-based methods (interferometry or deflection) require a certain thickness of the cantilever or a reflective coating to allow for enough reflectivity of the incident laser light. Coating the cantilever with a metal film, however, increases the thickness and, hence, the stiffness, as well as causes a reduction of the quality factor and an increase of low-frequency force noise [10]. This problem may be solved by the creation of a reflective spot only at the end of the beam but this requires additional steps in the cantilever fabrication process.

Furthermore, a certain cantilever width is necessary which led to the development of sophisticated structures with paddles either at or close to the cantilever end [11].

Additionally, other detection methods have been employed and successfully tested in the detection of the oscillatory state of nanocantilevers [12, 13]. However, all of these methods require sophisticated equipment and sometimes even low temperatures.

It is therefore a main challenge to develop a highly sensitive but easy to read-out cantilever sensor which would at best be compatible with the state-of-the-art laser-based detection methods.

Our recently developed co-resonant sensor concept addresses this challenge by coupling and eigenfrequency matching of a micro- and a nanocantilever. This approach gives access to a large fraction of the nanocantilever's high sensitivity while at the same time maintaining the ease of detection with a microcantilever. The concept has been tested in proof-of-principle experiments in cantilever magnetometry and magnetic force microscopy for various samples. In both cases the concept indicated an immense potential for the study of novel nanomaterials but also beyond. In the following we will first introduce the main ideas of the sensor concept and then present some results from the aforementioned experiments.

2 The co-resonant sensor concept

The sensor concept is based on the coupling of a micro- and a nanocantilever. The microcantilever has dimensions on the micrometer scale and therefore ensures the ease of

detection of the oscillatory state of the coupled system. The nanocantilever has at least a thickness of nanometer size, resulting in a very low stiffness and therefore a high sensitivity to external interactions as indicated by equation (2). Furthermore, the eigenfrequencies of both beams are brought close to one another (deviations typically less than 10 %) which induces a strong interplay between the two cantilevers and which will be denoted by co-resonance in the following. Consequently, this results in a coupled system where any interaction applied at the highly sensitive nanocantilever influences the oscillatory state of the coupled system as a whole. The change of the oscillatory state can be detected with state-of-the-art laser-based methods at the microcantilever. With this approach, a large portion of the nanocantilever's high sensitivity becomes accessible while maintaining the ease of detection [14].

2.1 System modelling

As mentioned above, a cantilever can be described by a harmonic oscillator model with different numerical values for each of its eigenfrequencies [8]. This model can also be applied to the co-resonantly coupled system, resulting in a coupled harmonic oscillator model as depicted in figure 1a. Furthermore, the external interaction can be included as an additional spring k_3 attached to the nanocantilever. k_3 represents an external force gradient and the derivation of this coherence can be found elsewhere, for example in [15].

In order to evaluate the sensor's behaviour, the amplitude response curves, especially of the microcantilever, are of interest because this is the quantity which is evaluated experimentally. These can be derived by solving the system of differential equations which describes the coupled harmonic oscillator model. These evaluations are very complex and it is therefore favorable to employ electro-mechanical analogies in order to use the capabilities of circuit analysis tools. The details of the circuit modelling are discussed in [16]. Here it suffices to state that the analogies force $F \equiv$ current I and velocity $v \equiv$ voltage U are used which preserve the structure of the mechanical model [17, 18, 19]. The resulting circuit model depicted in figure 1b is used for all subsequent simulations.

In the following discussion of the effects of the co-resonant coupling, the exemplary values listed in table 1 will be used for micro- and nanocantilever. They are comparable to values observed for actual sensors. Furthermore, we will only discuss the amplitude response curves for the microcantilever as these are the ones which are evaluated experimentally. However, please note that the
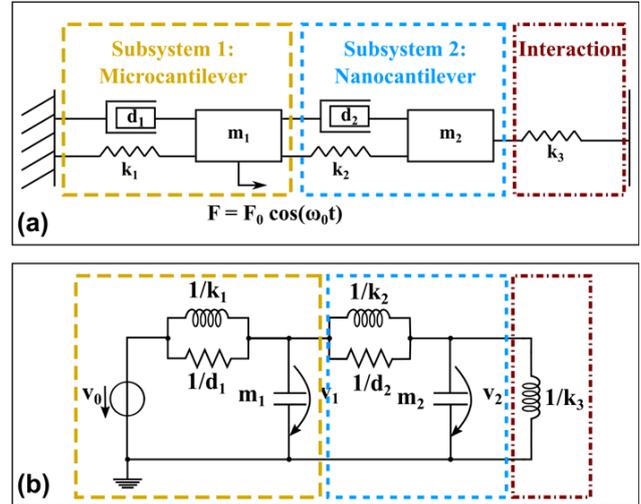

Figure 1: (a) Mechanical model of a coupled harmonic oscillator driven by a periodic force applied at the microcantilever and (b) corresponding electric circuit model. $d_{1,2}$, $k_{1,2}$ and $m_{1,2}$ are the beams' damping constant, spring constant and effective mass, respectively. The external interaction is modelled by an additional spring k_3.

Table 1: Exemplary values for micro- and nanocantilever used for the evaluation of the circuit model. Please note that the values are given for the individual subsystems in the unmatched frequency case. The quality factor of the nanocantilever is subject to change during eigenfrequency matching due to a change in effective nanocantilever mass.

Parameter	Microcant. (1)	Nanocant. (2)
Eigenfreq. f [Hz]	100000	variable
Spring const. k [N/m]	1	0.001
Quality factor Q	4000	500

same simulations and considerations are possible for the nanocantilever and can be found in [16].

In the following, it will be necessary to distinguish between the properties of the individual subsystems and the co-resonantly coupled system. Therefore, the former will be noted by the indexes $1, 2$ and the properties of the coupled system by indexes a, b.

2.2 Effect of frequency matching

To study the effect of frequency matching, the model from figure 1 is considered without the additional spring k_3. In the first case, we assume an unmatched frequency state, where the eigenfrequency of the microcantilever is $f_1 = 100\,\text{kHz}$ and that of the nanocantilever $f_2 = 200\,\text{kHz}$. The corresponding amplitude response curve for the micro-
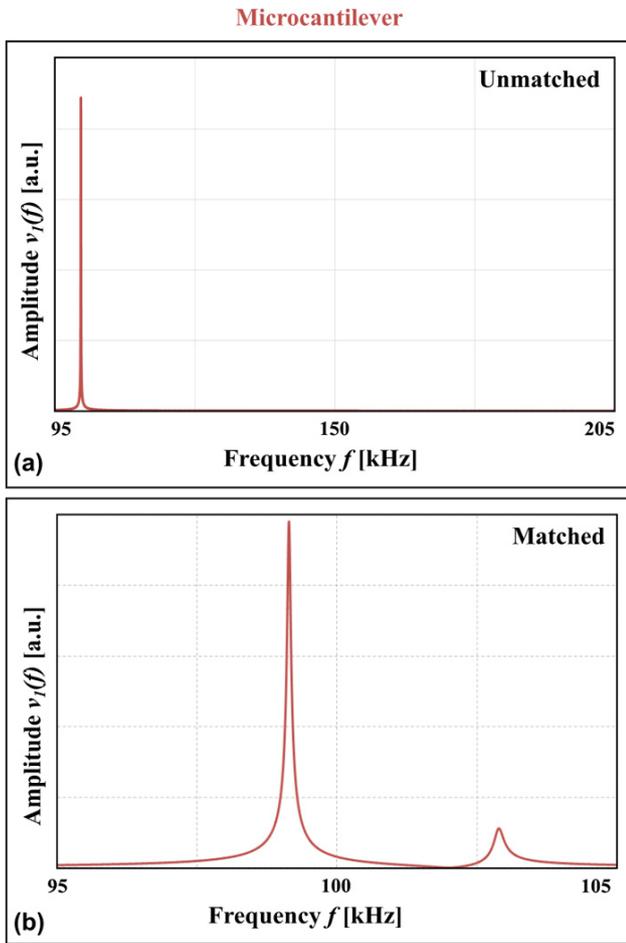
Microcantilever

(a)

(b)

Figure 2: Amplitude response curve of the microcantilever calculated for the values from table 1 with nanocantilever eigenfrequency of (a) 200 kHz and (b) 102 kHz (2 % frequency deviation).

Table 2: Numerical values for the two resonance frequencies $f_{a,b}$ of the coupled system in case of unmatched and matched (2 % deviation) eigenfrequencies $f_{1,2}$ of the individual beams. In both cases we assume ideal coupling of the two subsystems and only a change in the nanocantilever's eigenfrequency (matched or unmatched to the microcantilever) influences the resonance frequencies of the coupled system.

	Unmatched	Matched
f_1	100 kHz	100 kHz
f_2	200 kHz	102 kHz
f_a	99.984 kHz	99.142 kHz
f_b	200.032 kHz	102.890 kHz

cantilever is depicted in figure 2a and numerical values are listed in table 2. It exhibits one clear resonance peak very close to the eigenfrequency of the microcantilever. However, since it is a coupled system, a second resonance peak exists very close to the eigenfrequency of the nanocan-
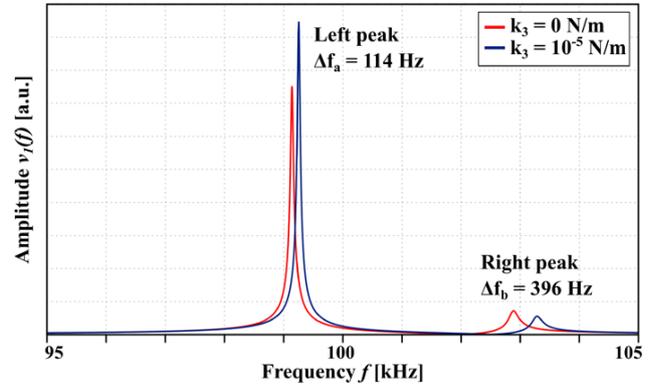

Figure 3: Amplitude response curve for the microcantilever in case for 2 % frequency deviation between the eigenfrequencies of micro- and nanocantilever with and without an interaction k_3. The frequency shift induced by the interaction is indicated for both resonance peaks.

tilever. The amplitude of the second peak is too small to be visible in the microcantilever's amplitude response curve due to the vastly different parameters of the subsystems.

This changes significantly in case of the eigenfrequency matching, where two clear resonance peaks are evident in the microcantilever's amplitude response curve (figure 2b). Furthermore, the resonance frequencies of the coupled system are clearly distinct from the individual beams' eigenfrequencies, indicating that they belong to the coupled system as a whole.

2.3 Effect of an interaction

Adding an interaction to the system, i. e. considering the complete model from figure 1, allows to study the influence of the co-resonance on the sensitivity of the system. The sensitivity S in this case can be defined as the frequency shift of the resonance peak Δf induced by an external force gradient $\Delta k = k_3$, hence $S = \Delta f / k_3$, and is dependent on the spring constant according to equation (2).

As an example, an interaction of $k_3 = 10^{-5}$ N/m was used in a simulation which is two orders of magnitude smaller than the smallest spring constant of the system. Figure 3 depicts the corresponding amplitude response curves for the microcantilever at 2 % frequency deviation between micro- and nanocantilever. It can clearly be seen that the frequency shift induced by k_3 is different for the two resonance peaks: the left-hand side peak with the higher amplitude shows a smaller frequency shift of $\Delta f_a = 144$ Hz compared to the peak with the smaller amplitude on the right $\Delta f_b = 396$ Hz.

To put that in perspective, the resulting frequency shifts are compared to those of the **individual** subsystems. The individual microcantilever has a frequency shift of $\Delta f_1 = 0.5$ Hz, while the individual nanocantilever shows a frequency shift of $\Delta f_2 = 509$ Hz. These values indicate that the coupled system's relevant sensor properties lie in between those of the individual beams. Furthermore, the resonance peak with the smaller amplitude is stronger influenced by the nanocantilever's properties, i. e. it exhibits a bigger frequency shift, while the peak with the larger amplitude is more dominated by the microcantilever's properties.

These considerations lead to effective parameters (spring constant, quality factor) in describing the behaviour of the two resonance peaks of the co-resonantly coupled system. Numerical values for the spring constants are $k_a = 0.0043$ N/m and $k_b = 0.0013$ N/m for the left and right peak, respectively. A comparison to $k_1 = 1$ N/m for the microcantilever and $k_2 = 0.001$ N/m for the nanocantilever demonstrates the effect of the co-resonant coupling on the spring constant and ultimately the sensitivity of the coupled system. It shows that a large fraction of the nanocantilever's low stiffness becomes accessible within the coupled state. Further analysis of these effective parameters, e. g. their dependence on the degree of frequency matching and the individual beams' parameters, is the subject of an ongoing study.

So far, we can conclude that the co-resonant coupling of a micro- and a nanocantilever gives access to a large portion of the nanocantilever's high sensitivity while at the same time preserving the ease of oscillation detection. Furthermore, the co-resonance leads to the necessity of effective parameters for describing the two resonance peaks of the coupled system.

3 Application in cantilever magnetometry

Cantilever magnetometry is a technique to study magnetic properties of samples. The sample is placed at the free end of a cantilever which is driven to resonant oscillations. The beam's oscillatory state (amplitude, phase and frequency) is commonly determined by focusing a laser beam at the cantilever's free end and detection of the reflected light with a sectioned photodiode or by interferometric means. Application of a static external magnetic field results in a magnetic interaction with the sample, inducing a restoring torque on the cantilever which alters the beam's oscillatory state. The change in oscillation properties can be related to the magnetic properties of the sample. In case of a *Stoner Wohlfarth* single domain ferromagnetic sample, the shift of the cantilever's resonance frequency can be approximated by [20, 21]:

$$\Delta f \approx \frac{\mu_0}{2} \frac{f_0}{k_0 L_{eff}^2} \cdot m \cdot \frac{H_{ext} H_a}{H_{ext} + H_a}. \tag{5}$$

The first part represents the sensor properties, i. e. resonance frequency without magnetic field f_0, spring constant k_0 and effective cantilever length $L_{eff} = L_{cant}/1.377$ [2]. The second part contains the sample properties which are magnetic moment m and anisotropy field H_a as well as the externally applied magnetic field H_{ext}. In order to measure small magnetic particles which only generate a weak magnetic interaction, the sensor has to be optimized. According to expression (5), a higher resonance frequency and shorter cantilever length are favorable. However, the tuning of these properties is limited as the reliable oscillation detection has to be ensured. Therefore, the main parameter for optimization is the spring constant. With the co-resonant approach, the low spring constant of a nanocantilever can be exploited as described in section 2.

3.1 Sensor geometry and fabrication

The co-resonant sensor geometry employed for cantilever magnetometry as well as a sketch of the resulting measurement setup are shown in figure 4a and d. A carbon nanotube (CNT) was used as nanocantilever due to its low spring constant and very good mechanical stability. The CNTs were grown by aerosol-assisted chemical vapor deposition [22], separated by ultrasonication and dispersed onto a TEM-grid. An individual CNT was transferred to the free end of a commercially available tipless silicon microcantilever (Nanosensors TL-CONT, *NanoWorld AG*) by micromanipulation and attached by electron beam-assisted material deposition (amorphous carbon), to achieve a mechanical coupling in series.

The eigenfrequencies of both beams were determined with a custom-made vibration stage inside a scanning electron microscope (SEM) by sweeping the excitation frequency and searching for the maximum oscillation amplitude (example in figure 4b). The microcantilever's eigenfrequency was measured before the attachment of the carbon nanotube and was assumed to only change minimally due to the coupling with the very light CNT. The nanocantilever's individual eigenfrequency was determined by 'decoupling' the system, i. e. by holding the microcantilever in place with the micromanipulator and therefore only driving the nanocantilever oscillation. Matching of the
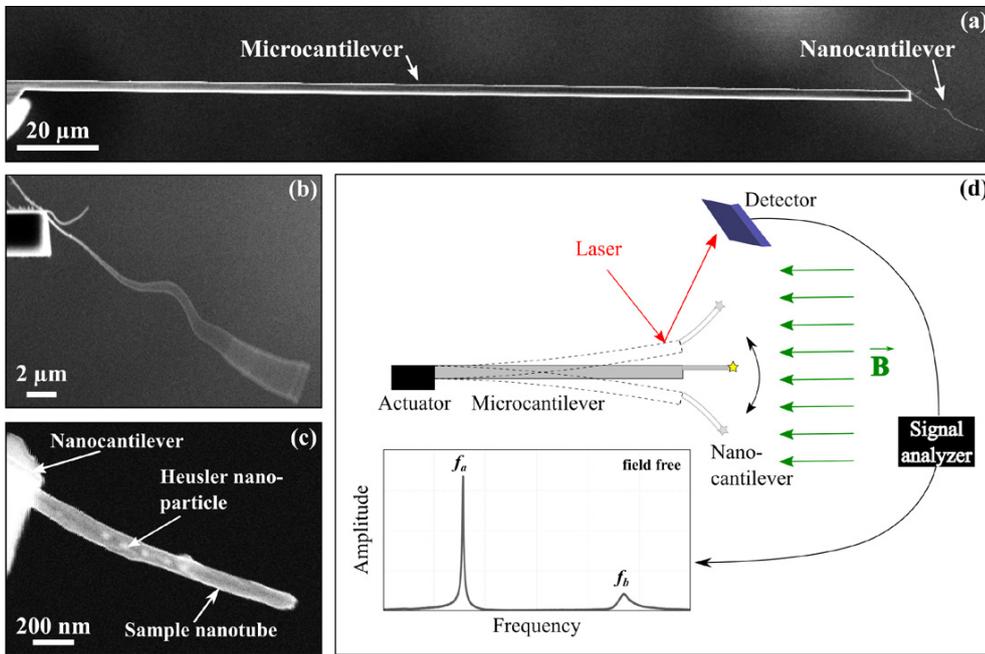
Figure 4: (a) SEM image of a co-resonantly coupled sensor consisting of a silicon microcantilever and a carbon nanotube nanocantilever, (b) exemplary oscillation of the nanocantilever, (c) free end of the nanocantilever with attached carbon nanotube containing few individual Co_2FeGa Heusler nanoparticles, (d) setup for co-resonant cantilever magnetometry. The amplitude response curve was measured for the sensor shown in (a).

eigenfrequencies was achieved by electron beam-assisted material deposition at the free end of the nanocantilever. The nanocantilever's oscillation was observed in the scanning electron microscope to ensure closely matched frequencies.

The sample was another carbon nanotube filled with few individual Co_2FeGa Heusler nanoparticles, which was placed at the free end of the nanocantilever by micromanipulation (see figure 4c). Heusler compounds are a class of intermetallic materials which feature very favorable transport and magnetic properties, making them candidates for prospective applications in spintronics, energy technology and thermoelectrics [23]. Detailed information about the fabrication process and the sample can be found in [24, 25, 26].

3.2 Results

Detailed results have been published in [24] and therefore only the key points will be summarized here.

All experiments were conducted under high vacuum and at room temperature with standard magnetic force microscope equipment which allowed for sensor excitation with a piezo-actor and oscillation detection via laser-deflection. The external magnetic field was applied through an electromagnet with variable field strength de-

pending on the electric current. The frequency shift for both resonance peaks of the coupled system was tracked with a phase-locked loop.

The frequency shift in dependence of the external magnetic field shows a hysteretic behaviour which can be expected for a ferromagnetic sample. However, when tracking the frequency shift of the smaller resonance peak (right-hand side peak f_b in figure 4d), distinct jumps in the frequency shift signal were observed. It is known from other magnetometry experiments that such jumps indicate the magnetization reversal of a magnetic sample [21]. In the aforementioned experiments we observed three clear jumps which we associate with the magnetization reversal of the biggest Heusler nanoparticles of our sample. It is unlikely that these jumps originated from thermal fluctuations or noise as they occurred reproducibly when the experiment was repeated at different times and on several days. Furthermore, the derived magnetic switching fields agree well with values reported in another study for ensembles of Heusler-filled carbon nanotubes [25, 26].

Besides the magnetic switching fields, an average magnetic moment, anisotropy field and particle aspect ratio (based on the demagnetization factors) could be derived by fitting the measured frequency shift data. A very good agreement is found between the values for both resonance peaks of the coupled system as well as with few other published experiments.

Consequently, these experiments indicate the immense potential of the co-resonantly coupled approach in cantilever magnetometry. We were, for the first time, able to observe magnetization reversal of individual Heusler nanoparticles at room temperature and with standard laser-deflection detection. Furthermore, we demonstrated that both resonance peaks of the coupled system strongly benefit from the high sensitivity of the nanocantilever.

4 Application in magnetic force microscopy

Besides cantilever magnetometry, the co-resonant sensor concept has been applied in magnetic force microscopy (MFM) to test its feasibility for this technique. The measurement setup is similar to cantilever magnetometry but in contrast to that, the cantilever is equipped with a magnetic interaction tip at its free end and the sample is placed underneath the beam on a xy-stage. The oscillating cantilever is scanned across the sample and the magnetic tip-sample interaction forces alter its oscillatory state. The change in amplitude, resonance frequency and/or phase is used to derive information about the magnetic stray field of sample, field gradients and topography.

Usually, the cantilever is driven to oscillate at its first flexural mode, i. e. the tip performs an up-and-down movement, which gives access to magnetic stray field gradients in the z-direction. Mühl et al. have developed a bi-directional scanning force microscopy concept which also allows the determination of magnetic stray field gradients in the in-plane direction, i. e. x and y [27, 28]. In that case, the cantilever is not driven at its first but at the second flexural vibration mode. This features a nodal point in the oscillation envelope which only exhibits an oscillating change of slope. When the magnetic interaction element is placed at this nodal point with some distance to the cantilever by means of a spacer element, the alternating change of slope is translated into a lateral movement of this element. With this approach, in-plane as well as out-of-plane stray field gradients are accessible since the cantilever can also be driven at its first flexural mode where the spacer element and interaction tip perform the common z-movement (see figure 5).

The co-resonant concept comes into play when an iron-filled carbon nanotube (FeCNT) is used as an interaction element and the eigenfrequency of the first flexural mode of the FeCNT is matched to the one of the second flexural mode of the microcantilever. In that case, the FeCNT is not a rigid interaction element anymore, but also performs
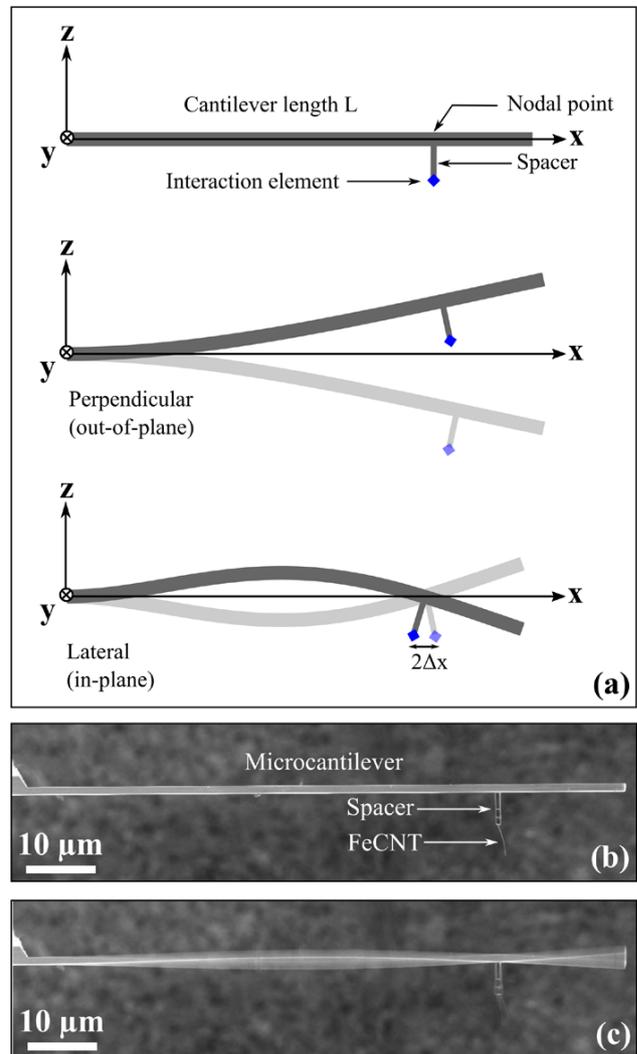

Figure 5: (a) Illustration of the bi-directional scanning force microscopy approach. The cantilever is equipped with a spacer element and an interaction tip at the position of the nodal point of its second flexural mode. This allows for the measurement of perpendicular (out-of-plane; 1st flexural mode) as well as lateral (in-plane; 2nd flexural mode) force gradients. (b) SEM image of an actual sensor consisting of a silicon microcantilever and a FeCNT as nanocantilever, thereby adding the possibility of co-resonant signal enhancement. (c) Co-resonantly enhanced oscillating sensor. The FeCNT is performing a resonant oscillation due to eigenfrequency matching of the second flexural mode of the microcantilever and first flexural mode of the FeCNT.

a resonant oscillation, leading to a tremendous increase in sensitivity [29, 30].

4.1 Experimental details

The sensor is fabricated by micromanipulation, focused ion beam and scanning electron beam techniques. First,

the oscillation of the microcantilever is measured with a vibration stage to determine its eigenfrequencies and identify the position of the nodal point (which can also be calculated). There, a pillar is grown by electron beam-assisted deposition of amorphous carbon. Finally, a FeCNT is attached to the end of the spacer element by micromanipulation and electron beam-assisted material deposition, with both long axes aligned. The eigenfrequency of the nanocantilever is determined again on the above-mentioned vibration stage in the SEM by holding the microcantilever with the micromanipulator, thereby decoupling the system. Frequency matching is achieved by material deposition at the free end of the FeCNT as for the cantilever magnetometry sensors [28].

The FeCNT is filled with a single magnetic domain iron core [31] so that effectively only the magnetic pole at the FeCNT's free end interacts with the sample's magnetic stray field and therefore constitutes a very defined monopole-like magnetic interaction [28].

By the co-resonant coupling, a system with effective parameters is created like in the case of cantilever magnetometry. Hence, the effective spring constant of the coupled system is drastically reduced compared to the individual microcantilever, resulting in a strongly increased sensitivity as demonstrated by the experimental results for a Co/Pt multilayer sample [29].

For these measurements, the co-resonantly coupled sensor was first excited at the first flexural mode of the microcantilever, performing a measurement of the perpendicular magnetic stray field gradient. In a second step, the measurement was repeated for the in-plane direction by driving the system at the co-resonantly enhanced second flexural mode of the microcantilever. Please note that this is one of the two resonance frequencies of the coupled system which are close to the second eigenfrequency of the microcantilever.

4.2 Results and discussion

The CoPt multilayer sample is a well-known system in terms of its magnetic domain structure and therefore it is possible to use the measured perpendicular, i. e. out-of-plane, stray field map to analytically calculate a theoretical in-plane stray field map with a Fourier transform-based approach. This calculation assumes a rigid carbon nanotube, i. e. no co-resonant signal enhancement. Details about these calculations can be found in [28, 32, 33].

The calculated image can be compared to the measured in-plane data obtained with the co-resonantly enhanced sensor. A line section for such a comparison is
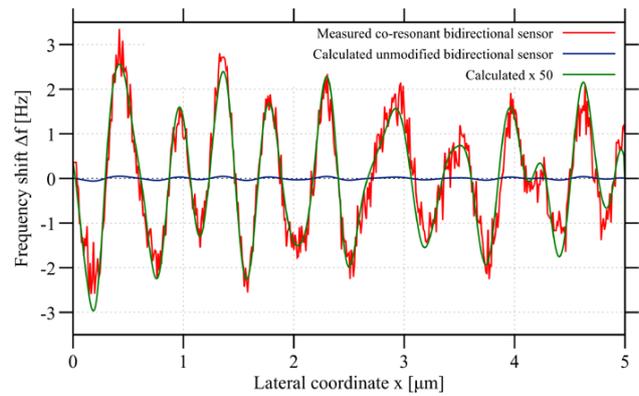

Figure 6: Line section of lateral operation mode frequency shift data measured on a Pt/Co multilayer sample with a bidirectional magnetic force microscopy sensor equipped with an FeCNT as interaction tip. The calculated lateral data is based on data of the same position measured with the same sensor in perpendicular operation mode assuming a rigid, i. e. not co-resonantly enhanced, carbon nanotube. Additionally this calculated data was multiplied by a factor of 50 to match the magnitude of the measured lateral data, thereby demonstrating the co-resonant signal enhancement.

depicted in figure 6. Please note that a Fourier filter was applied to the calculated data for increased clarity as the perpendicular, i. e. out-of-plane, experimental data and, therefore, the derived in-plane data had a low signal-to-noise ratio due to experimental limitations. The in-plane experimental data was used as measured.

Both line sections, for calculation and measurement, agree very well in terms of the curve shape. However, the calculated data had to be multiplied by a factor of approximately 50 to reach the same magnitude as the measured data. This is a direct consequence of the co-resonant coupling and demonstrates its immense potential for signal enhancement in this technique. Further experiments indicated an even higher signal enhancement by three to four orders of magnitude.

5 Conclusion

Finding ways to enhance the sensitivity of cantilever sensors is key for extending their application range for example as a means to study novel nanomaterials or as highly sensitive mass and gas sensors. The co-resonant sensor concept has the potential of creating such a highly sensitive sensor platform by coupling and eigenfrequency matching of a micro- and a nanocantilever. First experiments in the study of magnetic properties of samples in cantilever magnetometry and magnetic force microscopy demonstrated the huge potential of this approach. Further-

more, a theoretical basis for understanding and describing the behaviour of the co-resonantly coupled system has been established by mechanical and electric circuit modelling. Although not all implications are fully understood yet, it is very likely that many new applications based on that concept may evolve in the future, beyond material's research.

References

1. B. Gross, D. P. Weber, D. Rüffer, A. Buchter, F. Heimbach, A. Fontcuberta i Morral, D. Grundler and M. Poggio, Dynamic cantilever magnetometry of individual CoFeB nanotubes, *Physical Review B* 93(6) (2016), 064409.

2. U. Gysin, S. Rast, A. Aste, T. Speliotis, C. Werle and E. Meyer, Magnetic properties of nanomagnetic and biomagnetic systems analyzed using cantilever magnetometry, *Nanotechnology* 22(8) (2011), 285715.

3. D. Martínez-Martín, G. Fläschner, B. Gaub, S. Martin, R. Newton, C. Beerli, J. Mercer, C. Gerber and D. J. Müller, Inertial picobalance reveals fast mass fluctuations in mammalian cells, *Nature* 550 (2017), 500.

4. L. G. Carrascosa, M. Moreno, M. Álvarez and L. M. Lechuga, Nanomechanical biosensors: a new sensing tool, *Trends in Analytical Chemistry* 25(3) (2006), 196.

5. K. Y. Gfeller, N. Nugaeva and M. Hegner, Micromechanical oscillators as rapid biosensor for the detection of active growth of *Escherichia coli*, *Biosensors and Bioelectronics* 21 (2005), 528.

6. B. N. Johnson and R. Mutharasan, Biosensing using dynamic-mode cantilever sensors: A review, *Biosensors and Bioelectronics* 32 (2012), 1.

7. M. K. Baller, H. P. Lang, J. Fritz, C. Gerber, J. K. Gimzewski, U. Drechsler, H. Rothuizen, M. Despont, P. Vettiger, F. M. Battiston, J. P. Ramseyer, P. Fornardo, E. Meyer and H.-J. Güntherodt, A cantilever array-based artificial nose, *Ultramicroscopy* 82 (2000), 1.

8. S. Rast, C. Wattinger, U. Gysin and E. Meyer, Dynamics of damped cantilevers, *Review of Scientific Instruments* 71(7) (2000), 2772.

9. F. J. Giessibl, Advances in atomic force microscopy, *Review of Modern Physics* 75(3) (2003), 949.

10. Z. Schumacher, Y. Miyahara, L. Aeschimann and P. Grütter, Improved atomic force microscopy cantilever performance by partial reflective coating, *Beilstein Journal of Nanotechnology* 6 (2015), 1450.

11. D. P. Weber, D. Rüffer, A. Buchter, F. Xue, E. Russo-Averchi, R. Huber, P. Berberich, J. Arbiol, A. Fontcuberta i Morral, D. Grundler and M. Poggio, Cantilever Magnetometry of Individual Ni Nanotubes, *Nano Letters* 12(12) (2012), 6139.

12. E. Gil-Santos, D. Ramos, J. Martinez, M. Fernandez-Regulez, R. Garcia, A. San Paulo, M. Calleja and J. Tamayo, Nanomechanical mass sensing and stiffness spectrometry based on two-dimensional vibrations of resonant nanowires, *Nature Nanotechnology* 5 (2010), 641.

13. J. M. Nichol, E. R. Hemesath, L. J. Lauhin and R. Budakian, Displacement detection of silicon nanowires by polarization-enhanced fiber-optic interferometry, *Applied Physics Letters* 93 (2008), 193110.

14. C. F. Reiche, J. Körner, B. Büchner and T. Mühl, Introduction of a co-resonant detection concept for mechanical oscillation-based sensors, *Nanotechnology* 26(33) (2015), 335501.

15. T. D. Rossing and N. H. Fletcher, *Principles of Vibration and Sound*, 2 ed., Springer-Verlag, Berlin Heidelberg, 2004.

16. J. Körner, C. F. Reiche, B. Büchner, T. Mühl and G. Gerlach, Employing electro-mechanical analogies for co-resonantly coupled cantilever sensors, *Journal of Sensors and Sensor Systems* 5 (2016), 242.

17. A. Lenk, G. Pfeifer and R. Werthschützky, *Elektromechanische Systeme*, Springer-Verlag, Berlin Heidelberg, 2001.

18. W. Hähnle, Die Darstellung elektromechanischer Gebilde durch rein elektrische Schaltbilder, *Veröffentlichungen aus dem Siemens-Konzern* XI(1) (1931), 1–23.

19. K. Klotter, Die Analogien zwischen elektrischen und mechanischen Schwingern, *Ingenieur Archiv* 18(5) (1950), 291.

20. B. C. Stipe, H. J. Mamin, T. D. Stowe, T. W. Kenny and D. Rugar, Magnetic Dissipation and Fluctuations in Individual Nanomagnets Measured by Ultrasensitive Cantilever Magnetometry, *Physical Review Letters* 86(13) (2001), 2874.

21. P. Banerjee, F. Wolny, D. V. Pelekhov, M. R. Herman, K. C. Fong, U. Weissker, T. Mühl, Yu. Obukhov, A. Leonhardt, B. Büchner and C. Hammel, Magnetization reversal in an individual 25 nm iron-filled carbon nanotube, *Applied Physics Letters* 96 (2010), 252505.

22. S. S. Meysami, A. A. Koós, F. Dillon and N. Grobert, Aerosol-assisted chemical vapour deposition synthesis of multi-wall carbon nanotubes: II. an analytical study, *Carbon* 58 (2013), 159.

23. T. Graf, C. Felser and S. S. P. Parkin, Simple rules for the understanding of Heusler compounds, *Progress in Solid State Chemistry* 39(1) (2011), 1.

24. J. Körner, C. F. Reiche, R. Ghunaim, R. Fuge, S. Hampel, B. Büchner and T. Mühl, Magnetic properties of individual Co_2FeGa Heusler nanoparticles studied at room temperature by a highly sensitive co-resonant cantilever sensor, *Scientific Reports* 7 (2017), 8881.

25. M. Gellesch, *Statistical study of the effect of annealing treatments on assemblies of intermetallic magnetic nanoparticles related to the Heusler compound Co_2FeGa*, Ph.D. thesis, Fakultät Mathematik und Naturwissenschaften, Technische Universität Dresden, 2016.

26. M. Gellesch, M. Dimitrakopoulou, M. Scholz, C. G. F. Blum, M. Schulze, J. van de Brink, S. Hampel, S. Wurmehl and B. Büchner, Facile Nanotube-Assisted Synthesis of Ternary Intermetallic Nanocrystals of the Ferromagnetic Heusler Phase Co_2FeGa, *Crystal Growth and Design* 13(7) (2013), 2707.

27. T. Mühl, J. Körner, S. Philippi, C. F. Reiche, A. Leonhardt and
     B. Büchner, Magnetic force microscopy sensors providing
     in-plane and perpendicular sensitivity, *Applied Physics Letters*
     101(11) (2012), 112401.
28. C. F. Reiche, S. Vock, V. Neu, L. Schultz, B. Büchner and T. Mühl,
     Bidirectional quantitative force gradient microscopy, *New
     Journal of Physics* 17(1) (2015), 013014.
29. C. F. Reiche, *Novel Sensors for Scanning Force Microscopy
     Based on Carbon Nanotube Mechanical Resonators*, Ph.D.
     thesis, Fakultät Mathematik und Naturwissenschaften,
     Technische Universität Dresden, 2015.
30. C. F. Reiche, J. Körner, B. Büchner and T. Mühl, Bidirectional
     scanning force microscopy probes with co-resonant sensitivity
     enhancement, in: *Proceedings of the 15th IEEE International
     Conference on Nanotechnology, Rome*, p. 1222, 2015.
31. F. Wolny, U. Weissker, T. Mühl, A. Leonhardt, S. Menzel,
     A. Winkler and B. Büchner, Iron-filled carbon nanotubes as
     probes for magnetic force microscopy, *Journal of Applied
     Physics* 104(6) (2008), 064908.
32. S. Vock, C. Hengst, M. Wolf, K. Tschulik, M. Uhlemann,
     Z. Sasvári, D. Makarov, O. G. Schmidt, L. Schultz and V. Neu,
     Magnetic vortex observation in FeCo nanowires by quantitative
     magnetic force microscopy, *Applied Physics Letters* 105 (2014),
     172409.
33. S. Vock, *Resolving Local Magnetization Structures by
     Quantitative Magnetic Force Microscopy*, Ph.D. thesis, Fakultät
     Mathematik und Naturwissenschaften, Technische Universität
     Dresden, 2014.

Bionotes

Julia Körner
Leibniz Institute for Solid State and
Materials Research IFW Dresden,
Helmholtzstr. 20, 01069 Dresden, Germany
Department of Electrical and Computer
Engineering, University of Utah, 50 Central
Campus Dr Suite 2110, Salt Lake City,
UT-84112, USA
julia.koerner2k@gmail.com

Julia Körner studied electrical engineering at the Technical University Dresden and graduated in 2012 with a Diploma. She obtained her PhD in 2016 from the Technical University Dresden for a novel co-resonant cantilever sensor concept for cantilever magnetometry. This research was done at the IFW Dresden. Currently, she is research assistant professor at the University of Utah in Salt Lake City where she keeps working on co-resonantly coupled cantilever sensors and hydrogel-based sensors for biomedical applications.

Christopher F. Reiche
Leibniz Institute for Solid State and
Materials Research IFW Dresden,
Helmholtzstr. 20, 01069 Dresden, Germany
Department of Electrical and Computer
Engineering, University of Utah, 50 Central
Campus Dr Suite 2110, Salt Lake City,
UT-84112, USA
christopher.reiche@utah.edu

Christopher Reiche studied physics at the Karlsruhe Institute of Technology. After that he joined the IFW Dresden where he worked on novel magnetic force microscopy sensors and obtained his PhD in 2016 from the Technical University Dresden. He is currently employed as research associate at the University of Utah where he is pursuing research on hydrogel-based sensors for biomedical applications.

Bernd Büchner
Leibniz Institute for Solid State and
Materials Research IFW Dresden,
Helmholtzstr. 20, 01069 Dresden, Germany
Institut für Festkörperphysik, Technische
Universität Dresden, 01062 Dresden,
Germany
Center for Transport and Devices of
Emergent Materials, Technische Universität
Dresden, 01062, Dresden, Germany
B.buechner@ifw-dresden.de

Bernd Büchner is director of the Institute of Solid State Research at the IFW Dresden and professor for experimental physics at Technical University Dresden. His research focus is on superconductivity and magnetism in unconventional superconductors as well as on novel materials such as transition metal oxides, lanthanides, molecular nanostructures and molecular magnets. He has authored over 400 scientific publications.

Thomas Mühl
Leibniz Institute for Solid State and
Materials Research IFW Dresden,
Helmholtzstr. 20, 01069 Dresden, Germany
Center for Transport and Devices of
Emergent Materials, Technische Universität
Dresden, 01062, Dresden, Germany
t.muehl@ifw-dresden.de

Thomas Mühl studied physics at the Technical University Dresden where he also obtained his PhD. He is currently a group leader at the Leibniz Institute for Solid State and Materials Research IFW Dresden and his research focus is on scanning probe microscopy methods and nanomagnetism.